Investigation of LC-Hybrid Active Power Filters in Resonances Prevention and Compensation Capabilities

Chi-Seng Lam[1], Man-Chung Wong[1], Ying-Duo Han[1,2]
1 - Department of Electrical and Computer Engineering, University of Macau, Macau, SAR, P. R. China
2 - Department of Electrical Engineering, Tsinghua University, Beijing, P. R. China
E-mail: cslam@umac.mo

***Abstract*—This paper presents the harmonic resonances prevention and compensation capabilities of three-phase four-wire center-spilt LC coupling hybrid active power filter (LC-HAPF). Firstly, a single-phase harmonic equivalent circuit model of the LC-HAPF is deduced and built. Based on the circuit model, the LC-HAPF compensation characteristics are studied and analyzed in details, which shows a superior compensation characteristic compared with its pure passive power filter (PPF) part. Finally, simulation results for the pure PPF part and LC-HAPF are given to verify all the analyses.**

I. INTRODUCTION

Since the first installation of passive power filters (PPFs) in the mid 1940's, PPFs have been widely used to compensate current quality problems in distribution power systems [1] due to their low cost, simplicity and high efficiency. However, they have disadvantages such as low dynamic performance, resonance problems, etc. [2] – [5]. Since the concept "Active ac Power Filter" was first developed by L. Gyugyi in 1976 [1], [3], the research studies of the active power filters (APFs) are prospering since then. APFs can overcome the disadvantages inherent in PPFs, but their initial costs are relatively high [2] – [4] because the dc-link operating voltage should be higher than the system voltage. In order to lower the cost of APFs, different hybrid active power filter (HAPF) topologies have been proposed. The HAPF topologies in [2] – [5] consist of many passive components, thus increasing the whole system cost. A LC coupling HAPF (LC-HAPF) has been recently proposed for current quality compensation and harmonic damping [6] – [9], because it has less passive components and the dc-link operating voltage can be much lower than the APF.

In this paper, the compensating performances for a LC-HAPF and its PPF part will be studied, analyzed and compared with four evaluation indexes: capabilities to prevent parallel resonance, series resonance, improve the filtering performances and enhance the system robustness. Firstly, a single-phase harmonics equivalent circuit model of a three-phase four-wire center-spilt LC-HAPF is deduced and built. Based on the model, the compensation performances under either LC-HAPF or its pure PPF part operation will be studied. At last, their simulated current quality compensation results will be given to verify all the deduced and analyzed results.

II. ANALYSIS OF LC-HAPF COMPENSATION PERFORMANCES

A. LC-HAPF Single-phase Harmonic Circuit Model

Fig. 1 shows a three-phase four-wire center-spilt LC-HAPF, where the subscript 'x' denotes phase $x = a,b,c,n$. v_{sx} and v_x are the system and load voltage, L_s is the system inductance. i_{sx}, i_{Lx} and i_{cx} are the system, load and inverter current for each phase. C_{c1}, L_{c1} and R_{c1} are the coupling part capacitance, inductance and internal resistance. C_{dc1}, V_{dc1_U} and V_{dc1_L} are the dc capacitance, upper and lower dc capacitor voltages with $V_{dc1_U} = V_{dc1_L} = 0.5V_{dc1}$. From Fig. 1, the inverter line-to-ground voltages $v_{inv1x-g}$ will be equal to the inverter line-to-neutral voltages $v_{inv1x-n}$ because the neutral point n is connected to the dc-link midpoint g.

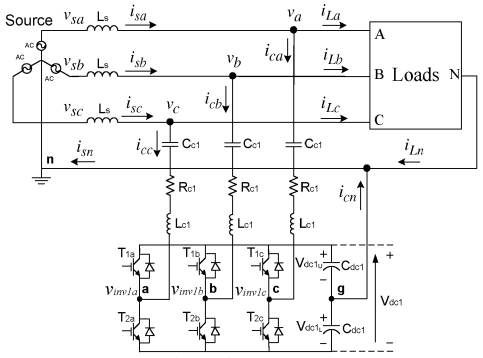

Figure 1. Configuration of a three-phase four-wire center-spilt LC-HAPF

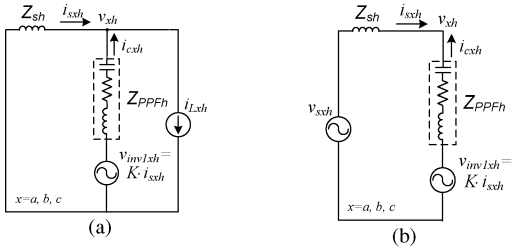

Figure 2. Simplified LC-HAPF single-phase harmonic circuit model: (a) when only i_{Lxh} is considered, (b) when only v_{sxh} is considered

Fig. 2 show the simplified LC-HAPF single-phase harmonic circuit model due to loading harmonic current i_{Lxh} and system harmonic voltage v_{sxh}, where the subscript "h" represents harmonic components. The loading and inverter are modeled as current and voltage sources. Z_{sh} and Z_{PPFh} are the harmonic impedance of the system and PPF part. Provided that the inverter is controlled by hysteresis PWM with hysteresis error band $H = 0$, the inverter can be modeled as a current control voltage source.

When $(i_{cxh}{}^* - i_{cxh}) \geq H$, i.e. $(i_{cxh}{}^* - i_{cxh}) \geq 0$,

$$v_{invx1h} = 0.5V_{dc1} = K_1 \cdot (i_{cxh}{}^* - i_{cxh}),\ K_1 > 0 \quad (1)$$

When $(i_{cxh}{}^* - i_{cxh}) < H$, i.e. $(i_{cxh}{}^* - i_{cxh}) < 0$,

$$v_{invx1h} = -0.5V_{dc1} = K_2 \cdot (i_{cxh}{}^* - i_{cxh}),\ K_2 > 0 \quad (2)$$

Where v_{invx1h} represents the inverter harmonic output voltage, $i_{cxh}{}^*$ and i_{cxh} represent the reference and actual harmonic compensating currents. Since K_1 and K_2 are both in positive, v_{invx1h} can be expressed into a general form as:

$$v_{invx1h} = K \cdot (i_{cxh}{}^* - i_{cxh}),\ K > 0 \quad (3)$$

From Fig. 2, $i_{sxh} + i_{cxh} = i_{Lxh}$. In ideal compensation case, $i_{cxh}{}^* = i_{Lxh}$. Thus, v_{invx1h} can also be expressed as:

$$v_{inv1xh} = K \cdot i_{sxh},\ K > 0 \quad (4)$$

B. LC-HAPF Harmonic Circuit Model Due to i_{Lxh} only

For the system voltage v_{sx} does not contain harmonic components ($v_{sxh} = 0$), the LC-HAPF single-phase harmonic circuit model due to i_{Lxh} is shown in Fig. 2(a). From Fig. 2(a), the i_{sxh} and i_{cxh} due to i_{Lxh} only can be expressed as:

$$K_{sxh\_i} = \frac{i_{sxh}}{i_{Lxh}} = \frac{Z_{PPFh}}{K + Z_{sh} + Z_{PPFh}} \quad (5)$$

$$K_{cxh\_i} = \frac{i_{cxh}}{i_{Lxh}} = \frac{K + Z_{sh}}{K + Z_{sh} + Z_{PPFh}} \quad (6)$$

In a perfect compensation, $K_{sxh\_i} = 0$ and $K_{cxh\_i} = 1$ should be achieved so that all the load harmonic current flows into the LC-HAPF ($i_{cxh} = i_{Lxh}$). In order to achieve this objective, K should be a large value.

C. LC-HAPF Harmonic Circuit Model Due to v_{sxh} only

For the load current i_{Lx} does not contain harmonic components ($i_{Lxh} = 0$), the LC-HAPF single-phase harmonic circuit model due to v_{sxh} is shown in Fig. 2(b). From Fig. 2(b), the i_{sxh} and i_{cxh} due to v_{sxh} only can be expressed as:

$$K_{sxh\_v} = \frac{i_{sxh}}{v_{sxh}} = \frac{1}{K + Z_{sh} + Z_{PPFh}} \quad (7)$$

$$K_{cxh\_v} = \frac{i_{cxh}}{v_{sxh}} = -\frac{1}{K + Z_{sh} + Z_{PPFh}} \quad (8)$$

Similarly, in order to achieve $K_{sxh\_v} = 0$, K should also be a large value. From (5) – (8), when only the pure PPF part is employed, $K = 0$.

D. Investigation of LC-HAPF Compensation Performances

In the following, the LC-HAPF steady-state compensating performances are studied and discussed with four evaluation indexes, compared with those of the pure PPF part. Table I shows a set of LC-HAPF system parameters for the analyses.

TABLE I. A SET OF LC-HAPF SYSTEM PARAMETERS

System Parameters	Physical Values
v_x	$220V_{rms}$
L_s, L_{c1}	1mH, 5mH
C_{c1}, R_{c1}	80μF, 0Ω
V_{dc1_U}, V_{dc1_L}	50V

1) LC-HAPF Capability to Prevent Parallel Resonance

Fig. 3 shows the K_{sxh_i} (5) diagram with respect to different frequency and L_s when the PPF part or LC-HAPF is utilized. When only pure PPF is used ($K = 0$), the harmonic current amplification phenomenon occurs. When the LC-HAPF is employed, the parallel resonance phenomenon disappears. Fig. 3 shows that the LC-HAPF has the ability to prevent the parallel resonance inherent in the pure PPF part.

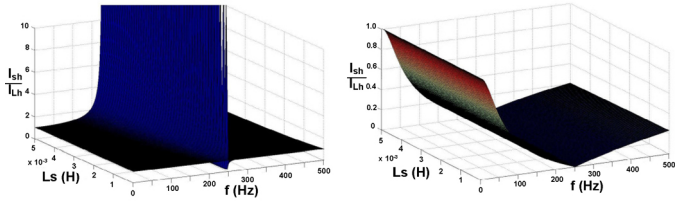

(a) (b)

Figure 3. Capability to prevent parallel resonance: (a) only PPF part is utilized ($K = 0$), (b) LC-HAPF is employed ($K = 50$)

2) LC-HAPF Capability to Prevent Series Resonance

Fig. 4 shows the K_{cxh_v} (8) diagram with respect to different frequency and L_s when the PPF part or LC-HAPF is utilized. When only pure PPF is used ($K = 0$), the harmonic current amplification phenomenon occurs. When the LC-HAPF is employed, the series resonance phenomenon disappears. Fig. 4 shows that the LC-HAPF has the ability to prevent the series resonance inherent in the pure PPF part.

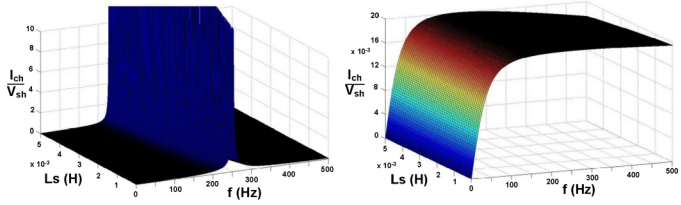

(a) (b)

Figure 4. Capability to prevent series resonance: (a) only PPF part is utilized ($K = 0$), (b) LC-HAPF is employed ($K = 50$)

3) LC-HAPF Capability to Improve Filtering Performances

Fig. 5 shows the bode diagrams of K_{sxh_i} (5) and K_{sxh_v} (7) with respect to different K. When only pure PPF is used ($K = 0$), the harmonic current amplification phenomenon occurs at $\omega = 1120$ rad/s. When the LC-HAPF is employed

($K = 25$ or $K = 50$), K_{sxh_i} and K_{sxh_v} will have a larger attenuation at different harmonic frequencies. Fig. 5 shows the LC-HAPF is capable to improve the filtering performances.

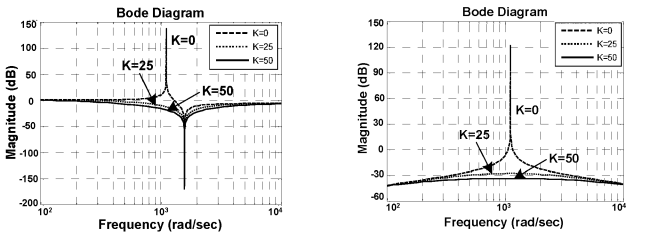

(a) (b)

Figure 5. Capability to improve the filtering performances of the PPF part ($K = 0$, $K = 25$, $K = 50$) due to: (a) i_{Lxh} , (b) v_{sxh}

4) LC-HAPF Capability to Enhance System Robustness

Fig. 6 shows the bode diagrams of K_{sxh_i} (5) with respect to different L_s . When only pure PPF is used ($K = 0$), the harmonic current amplification phenomenon will move to the lower frequency side as L_s increases. When the LC-HAPF is used ($K = 50$), the harmonic current amplification effect disappears no matter what L_s value is. Also, its harmonic compensating characteristics does not vary at all. Fig. 6 shows the LC-HAPF is capable to enhance the system robustness.

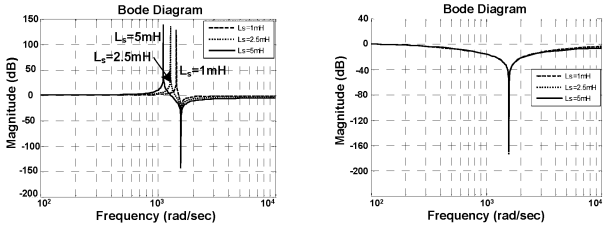

(a) (b)

Figure 6. Capability to enhance the system robustness: (a) only PPF part is utilized ($K = 0$), (b) LC-HAPF is employed ($K = 50$)

III. Simulation Verification

In this section, simulation results are included to illustrate and verify the previous LC-HAPF compensation performance analyses. Simulation studies were carried out using PSCAD/EMTDC. Table I shows the LC-HAPF simulated system parameters for balanced loading current quality compensation. Based on the instantaneous power theory [10], the control block diagram for the LC-HAPF is shown in Fig. 7.

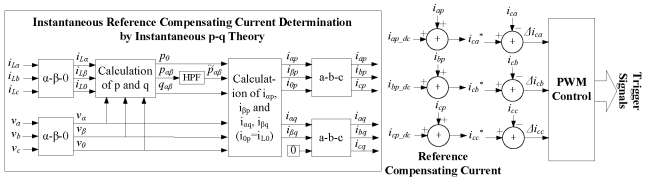

Figure 7. Control block diagram for the three-phase four-wire LC-HAPF

1) LC-HAPF Capability to Prevent Parallel Resonance

Fig. 8 shows the capability to prevent parallel resonance phenomenon: (a) only PPF part is utilized, (b) LC-HAPF is employed. When L_s increases to 5mH, the parallel resonance will occur close to the 3rd order harmonic frequency as shown in Fig. 3(a). Fig. 8(a) shows that the pure PPF compensation amplifies the 3rd order harmonic from 2.00A_{rms} to 4.59A_{rms}. This phenomenon deteriorates the compensation results as shown in Table II, in which $THD_{i_{sx}}$ and THD_{v_x} do not satisfy the international standards [11]–[13]. When the LC-HAPF is employed, Fig. 8(b) and Table II show that the LC-HAPF can obtain good compensation results without parallel resonance, which verified the parallel resonance analysis as in Fig. 3.

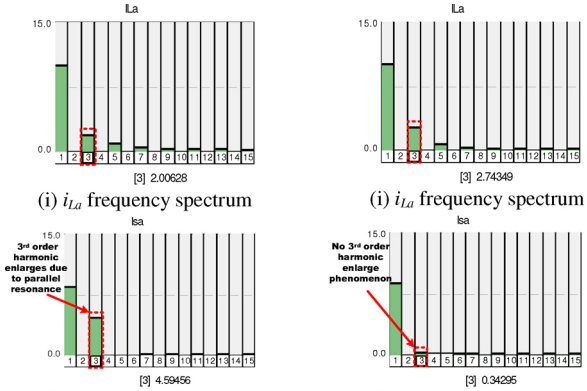

(i) i_{La} frequency spectrum (i) i_{La} frequency spectrum

(ii) i_{sa} frequency spectrum (ii) i_{sa} frequency spectrum

(a) (b)

Figure 8. Capability to prevent parallel resonance: (a) only PPF part is utilized, (b) LC-HAPF is employed

2) LC-HAPF Capability to Prevent Series Resonance

Fig. 9 shows the capability to prevent series resonance phenomenon: (a) only PPF part is utilized, (b) LC-HAPF is employed. Since L_{c1} and C_{c1} are tuned at 5th order, the series resonance will occur when 5th order system harmonic voltage presents, as shown in Fig. 4(a). When 4% of 5th order system harmonic voltage is added, Fig. 9(a) shows that the pure PPF operation will yield a series resonance with 5th order harmonic content increases from 0.74A_{rms} to 5.94A_{rms}. This phenomenon deteriorates the compensation results as illustrated in Table II, in which $THD_{i_{sx}}$ and THD_{v_x} do not satisfy the international standards [11]–[13]. When the LC-HAPF is employed, Fig. 9(b) and Table II show that the LC-HAPF can obtain good compensation results without series resonance, which verified the series resonance analysis as in Fig. 4.

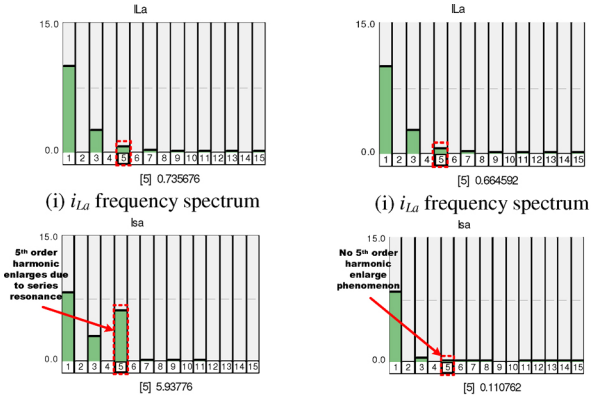

(i) i_{La} frequency spectrum (i) i_{La} frequency spectrum

(ii) i_{sa} frequency spectrum (ii) i_{sa} frequency spectrum

(a) (b)

Figure 9. Capability to prevent series resonance: (a) only PPF part is utilized, (b) LC-HAPF is employed

3) LC-HAPF Capability to Improve Filtering Performances

Fig. 10 shows the capability to improve the filtering performances: (a) only PPF part is utilized, (b) LC-HAPF is employed. From Fig. 10(a), when only PPF is employed, the i_{sx} fundamental and 5th order harmonic content have been reduced. But it yields a larger $THD_{i_{sx}}$ of 37.0% as shown in Table II, in which $THD_{i_{sx}}$ does not satisfy the international standards [11]–[13]. When the LC-HAPF is employed, Fig. 10(b) and Table II show that the LC-HAPF can obtain good compensation performances, which verified the filtering improvement analysis as in Fig. 5.

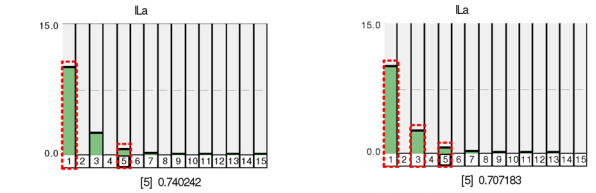

(i) i_{La} frequency spectrum (i) i_{La} frequency spectrum

(ii) i_{sa} frequency spectrum (ii) i_{sa} frequency spectrum

(a) (b)

Figure 10. Capability to improve the filtering performances of the PPF part: (a) only PPF part is utilized, (b) LC-HAPF is employed

4) LC-HAPF Capability to Enhance System Robustness

Fig. 11 shows the capability to enhance the system robustness: (a) only the PPF part is utilized, (b) LC-HAPF is employed. When L_s changes to 3mH, the compensating characteristics are being changed as shown in Fig. 6(a). Fig. 11(a) shows that the PPF part amplifies the i_{sx} 3rd order harmonic content. This deteriorates the compensation results, in which $THD_{i_{sx}}$ and THD_{v_x} do not satisfy the standards [11]–[13]. When the LC-HAPF is employed, Fig. 11(b) and Table II show the LC-HAPF can perform good compensation, which verified the system robustness analysis as in Fig. 6.

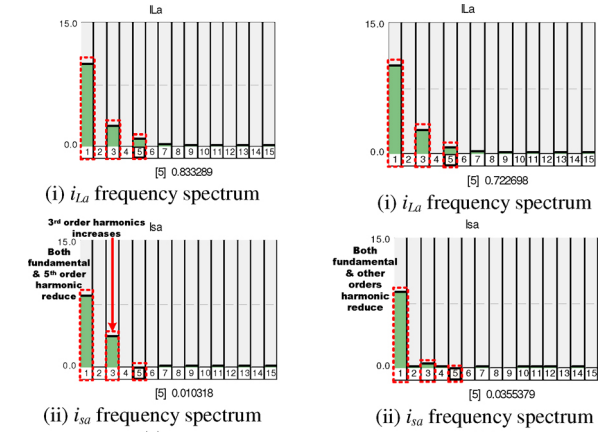

(i) i_{La} frequency spectrum (i) i_{La} frequency spectrum

(ii) i_{sa} frequency spectrum (ii) i_{sa} frequency spectrum

(a) (b)

Figure 11. Capability to enhance the system robustness: (a) only PPF part is utilized, (b) LC-HAPF is employed

TABLE II. SIMULATION RESULTS BEFORE AND AFTER PPF AND LC-HAPF COMPENSATIONS

Capabilities		Before Compensation			After Compensation			
		$THD_{i_{sx}}$ (%)	i_{sn} (A_{rms})	DPF	$THD_{i_{sx}}$ (%)	i_{sn} (A_{rms})	DPF	THD_{v_x} (%)
Parallel Resonance	PPF	22.0	5.84	0.845	54.5	13.83	0.998	10.5
	LC-HAPF	30.0	8.56	0.838	5.6	1.16	1.000	4.8
Series Resonance	PPF	30.0	8.10	0.838	> 75.0	9.25	0.999	5.2
	LC-HAPF	30.0	8.56	0.838	8.5	1.17	1.000	4.6
Improve Filtering	PPF	30.0	8.10	0.838	37.0	9.30	1.000	2.1
	LC-HAPF	30.0	8.56	0.838	5.0	0.90	1.000	2.2
System Robustness	PPF	25.4	6.86	0.837	44.0	10.20	0.999	5.5
	LC-HAPF	30.0	8.56	0.838	5.2	1.05	1.000	4.0

IV. CONCLUSION

In this paper a single-phase harmonic circuit model of a three-phase four-wire center-spilt LC-HAPF is deduced and built. Based on the model, the steady-state compensating performances for pure PPF part and LC-HAPF are discussed and analyzed with four evaluation indexes, capabilities to prevent parallel resonance and series resonance, improve the filtering performances and enhance the system robustness. It is clearly illustrated that the LC-HAPF has the capabilities to prevent parallel and series resonance phenomena inherent in pure PPF part, improve the filtering effects and enhance the system robustness of the PPF part, in which all the deduced and analyzed results are verified by simulations.

REFERENCES

[1] S. T. Senini, and P.J. Wolfs, "Systematic identification and review of hybrid active filter topologies," in *Proc. IEEE 33rd Annual Power Electronics Specialists Conf., PESC. 02*, vol. 1, 2002, pp. 394–399.

[2] H. Fujita, and H. Akagi, "A practical approach to harmonic compensation in power systems – series connection of passive and active filters," *IEEE Trans. Ind. Applicat.*, vol. 27, pp. 1020–1025, Nov./Dec. 1991.

[3] F. Z. Peng, H. Akagi, and A. Nabae, "A new approach to harmonic compensation in power systems – a combined system of shunt passive and series active filters," *IEEE Trans. Ind. Applicat.*, vol. 26, pp. 983–990, Nov./Dec. 1990.

[4] S. Park, J.-H. Sung, and K. Nam, "A new parallel hybrid filter configuration minimizing active filter size," in *Proc. IEEE 30th Annual Power Electronics Specialists Conf., PESC. 99*, vol. 1, 1999, pp. 400–405.

[5] D. Rivas, L. Moran, J.W. Dixon, et al., "Improving passive filter compensation performance with active techniques," *IEEE Trans. Ind. Electron.*, vol. 50, pp. 161–170, Feb. 2003.

[6] S. Srianthumrong, H. Akagi, "A medium-voltage transformerless AC/DC Power conversion system consisting of a diode rectifier and a shunt hybrid filter," *IEEE Trans. Ind. Applicat.*, vol.39, pp.874 – 882, May/Jun. 2003.

[7] W. Tangtheerajaroonwong, T. Hatada, K. Wada, H. Akagi, "Design and performance of a transformerless shunt hybrid filter integrated into a three-phase diode rectifier," *IEEE Trans. Power Electron.*, vol. 22, pp. 1882–1889, Sept. 2007.

[8] H. -L. Jou, K. -D. Wu, J.- C. Wu, C. -H. Li, M. -S. Huang, "Novel power converter topology for three phase four-wire hybrid power filter," *IET Power Electron.*, vol.1, pp. 164 – 173, 2008.

[9] R. Inzunza, H. Akagi, "A 6.6-kV transformerless shunt hybrid active filter for installation on a power distribution system," *IEEE Trans. Power Electron.*, vol. 20, pp. 893 – 900, Jul. 2005.

[10] H. Akagi, S. Ogasawara, Kim Hyosung, "The theory of instantaneous power in three-phase four-wire systems: a comprehensive approach," *in Conf. Rec. IEEE-34th IAS Annu. Meeting*, 1999, vol. 1, pp. 431–439.

[11] IEEE Recommended Practices and Requirements for Harmonic Control in Electrical Power Systems, 1992, IEEE Standard 519-1992.

[12] IEEE Recommended Practice on Monitoring Electric Power Quality, 1995, IEEE Standard 1159:1995.

[13] Electromagnetic Compatibility (EMC), Part 3: Limits, Section 2: Limits for Harmonics Current Emissions (Equipment Input Current ≤16A Per Phase), IEC Standard 61000-3-2, 1997.